proceedings

Abstract

Use of infrared thermography for inspection of tensile deformation of Ti-25Nb-0.5O and Ti-25Nb-0.5N shape memory alloys†

Karol M. Golasiński [1,*], Michał Maj [2], Sandra Musiał [2], Wataru Tasaki [3] and Hee Young Kim [3]

[1] Cardinal Stefan Wyszynski University in Warsaw, Multidisciplinary Research Center, Dewajtis 5, 01-815 Warsaw, Poland; k.golasinski@uksw.edu.pl
[2] Institute of Fundamental Technological Research, Polish Academy of Sciences, Pawińskiego 5b, 02-106 Warsaw, Poland; mimaj@ippt.pan.pl; smusial@ippt.pan.pl
[3] Department of Materials Science, Institute of Pure and Applied Sciences, University of Tsukuba, Tsukuba, Ibaraki 305-8573, Japan; tasaki.wataru.fw@u.tsukuba.ac.jp; heeykim@ims.tsukuba.ac.jp

* Correspondence: k.golasinski@uksw.edu.pl
† Presented at the 18th International Workshop on Advanced Infrared Technology and Applications (AITA) 2025, in Kobe, Japan.

Keywords: shape memory alloys; interstitials; infrared thermography; digital image correlation.

The stress or temperature-induced martensitic transformation from the cubic β phase to the orthorhombic α'' phase is responsible for superelasticity or shape memory effect in the Ni-free Ti-based shape memory alloys (SMAs) [1-2]. However, the addition of the oxygen and nitrogen interstitials changes tensile characteristics of these SMAs [3-5]. For instance, the Ti–25Nb (at.%) SMA exhibits shape memory effect and a Lüders-type deformation, whereas oxygen-added Ti-25Nb based SMAs present different but still inhomogeneous superelastic deformation [6]. The goal of this work is to compare the thermomechanical behavior of two SMAs, with compositions Ti–25Nb–0.5O and Ti–25Nb–0.5N, subjected to load-unload tension.

The alloys were prepared by Ar arc melting method using pre-melted sponges of Ti (purity: >99.7%) and pure Nb (purity: 99.9%). The oxygen and nitrogen concentrations of the alloys were adjusted by amount of TiO2 and TiN powders (purity: 99.9%), respectively. Further processing included selected heat treatments and cold rolling specified in [1]. The load-unload tension was performed using an MTS 858 testing machine at strain rate of around 0.02 1/s. The gauge area of the specimen was 6 mm x 4 mm. During the experiments, a ThermaCam Phoenix camara, with high thermal sensitivity up to 0.02 K and the recording frequency of 200 Hz, was used to investigate thermal effects accompanying deformation of the Ti–25Nb–0.5O and Ti–25Nb–0.5N SMAs. Simultaneously, a sCMOS PCO Edge 5.5 camera was used to record a sequence in a visible spectrum for further processing using digital image correlation (DIC) to determine kinematic fields of these alloys in tension. The camera setting were as follows: the image size 931 pixels × 1280 pixels what gave pixel size equal to 7.7 μm, the recording frequency of the camera was equal to 100 Hz. An open source 2D digital image correlation program Thermocorr was used also to couple temperature fields. More details on the methodology are given in [7]. Examples of the experimental results obtained for Gum Metal (Ti–23Nb–0.7Ta–2.0Zr–1.2O; at.%) using this approach can be found in [8, 9].

Temperature ΔT and strain ε_{yy} fields of Ti–25Nb–0.5O and Ti–25Nb–0.5N SMAs under load–unload tension captured at specific stages of deformation identified in the

Citation: To be added by editorial staff during production.

Academic Editor: Firstname Lastname

Published: date

stress and temperature change vs. strain curves are shown in Figures 1(a) and 1(b), respectively. Stress-strain plots of the Ti–25Nb–0.5O and Ti–25Nb–0.5N SMAs show hysteretic behaviors characterized by superelasticity with the same recovery strains ε_r = 2%. However, the hysteresis loop is notably narrower in the case of the Ti–25Nb–0.5N SMA. Letters marked in the stress and temperature vs. strain curves correspond to the following instants of tension: $A_{O/N}$ and $A^*_{O/N}$ - stress σ_{tr} at minimum temperature ΔT_{min}; $B_{O/N}$ and $B^*_{O/N}$ - maximum stress σ_{max} and maximum temperature ΔT_{max}; $C_{O/N}$ and $C^*_{O/N}$ - σ = 0 MPa and temperature after unloading ΔT_{un}. Subscripts O and N refer to the SMAs doped with oxygen and nitrogen, respectively. During the loading, first the average temperature decreases due to the thermoelastic effect 0 - $A^*_{O/N}$ and with further loading the temperature significantly increases due to the forward stress-induced phase transformation $A^*_{O/N}$ - $B^*_{O/N}$. In the case of SMAs, ΔT_{min} can be an indicator of the transformation stress σ_{tr}. During unloading, first the temperature significantly decreases due to the reverse stress-induced phase transformation and at the final stage the temperature slightly increases due to the thermoelastic effect $B^*_{O/N}$ - $C^*_{O/N}$.

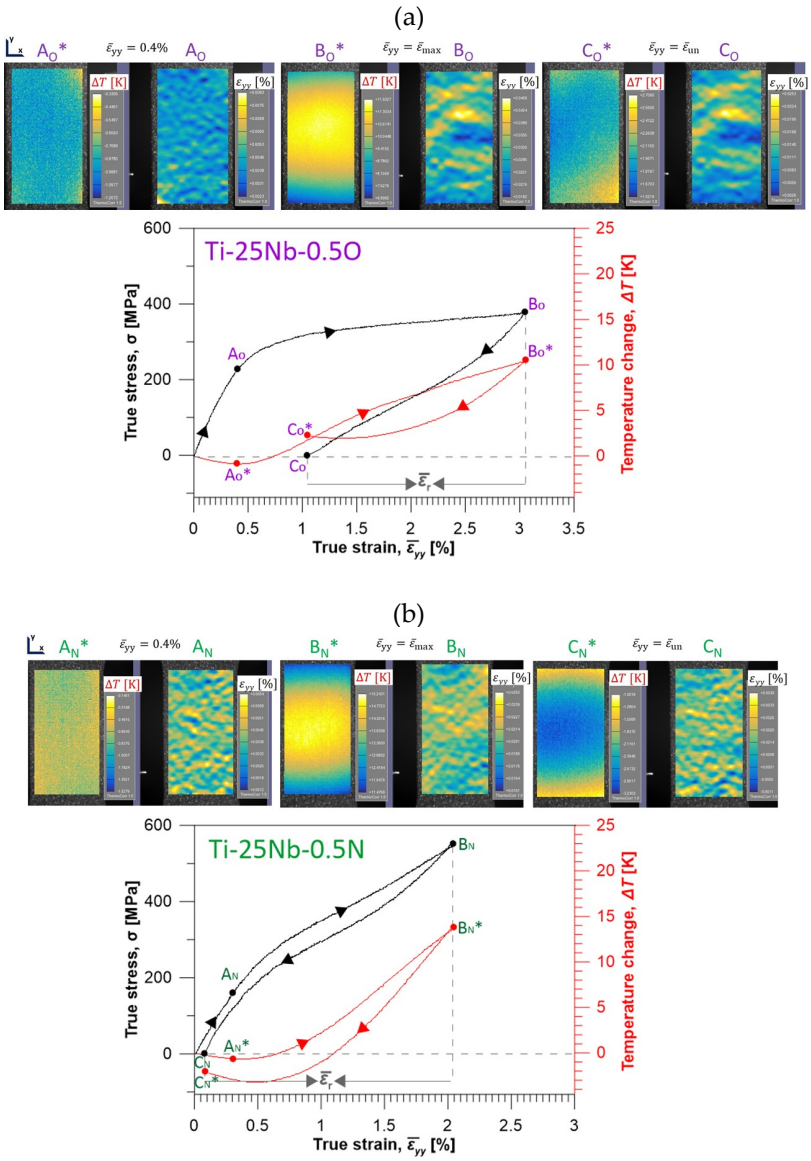

Figure 1. Temperature ΔT and strain ε_{yy} fields of (a) Ti–25Nb–0.5O and (b) Ti–25Nb–0.5N SMAs under load–unload tension at specific stages of deformation selected in the stress and temperature change vs. strain curves.

Although the strain rate applied during the experiments was relatively high to imitate adiabatic conditions, the heat exchange with the surroundings could slightly affect the results. Moreover, the aforementioned deformation mechanisms are believed to be dominant during specific stages of tension. However, in this class of alloys deformation twinning could also occur, especially in the final stage of loading, similarly to other metastable β-Ti alloys [10].

Critical parameters identified based on the stress and temperature change vs. strain curves of the Ti–25Nb–0.5O and Ti–25Nb–0.5N SMAs are listed in Table 1. They include transformation stress σ_{tr} at minimum temperature ΔT_{min} as well as temperature increase during loading ΔT_{eH} and temperature decrease ΔT_{eC} during unloading.

Table 1. Critical parameters identified based on the stress and temperature change vs. strain curves of the Ti–25Nb–0.5O and Ti–25Nb–0.5N SMAs.

Composition	Minimum temperature, ΔT_{min}	Transformation stress, σ_{tr}	Temperature increase, ΔT_{eH}	Temperature decrease, ΔT_{eC}
Ti-25Nb-0.5O	-0.89 K	236 MPa	11.34 K	8.42 K
Ti-25Nb-0.5N	-0.66 K	204 MPa	14.63 K	16.32 K

Temperature ΔT and strain ε_{yy} fields captured at selected instants of tension demonstrate that the deformation process was inhomogeneous. Maximum local values of ΔT_{max} and ε_{yy_max} determined at $B^*_{O/N}$ and $B_{O/N}$, respectively, are given in Table 2.

Table 2. Maximum local values of ΔT_{max} and ε_{yy_max} determined at $B^*_{O/N}$ and $B_{O/N}$.

Composition	Maximum local temperature, ΔT_{max}	Maximum local strain, ε_{yy_max}
Ti-25Nb-0.5O	11.93 K	4.6
Ti-25Nb-0.5N	15.24 K	2.5

The values of ΔT_{max} were rather close to those of ΔT_{eH}. However, the values of ε_{yy_max} were quite higher than those of $\varepsilon_{r.}$

Our results show that infrared thermography is a useful technique to track peculiar temperature changes of the Ti–25Nb–0.5O and Ti–25Nb–0.5N SMAs. The temperature fields captured at selected stages of loading revealed heat sources associated with deformation process. The thermal effects were discussed in view of the kinematic characteristics obtained using DIC. It was shown, that temperature change can serve to identify particular deformation stages of the SMAs considered in this study.

Author Contributions: Conceptualization, K.M.G. and H.Y.K.; methodology, K.M.G., M.M., S.M., W.T. and H.Y.K.; software, K.M.G., M.M. and S.M.; validation, X.X., Y.Y. and Z.Z.; formal analysis, X.X.; investigation, K.M.G., M.M. and S.M.; resources, K.M.G. and H.Y.K.; data curation, K.M.G., M.M. and S.M.; writing—original draft preparation, K.M.G.; writing—review and editing, K.M.G.; visualization, K.M.G., M.M. and S.M.; supervision, H.Y.K.; project administration, K.M.G. and H.Y.K.; funding acquisition, K.M.G. and H.Y.K. All authors have read and agreed to the published version of the manuscript.

Funding: Karol M. Golasiński acknowledges the support of the Japan Society for the Promotion of Science (JSPS) Postdoctoral Fellowship ID No. P20812. This research was funded by the National Science Centre, Poland through the Grant 2023/48/C/ST8/00038.

Institutional Review Board Statement: Not applicable.

Informed Consent Statement: Not applicable.

Data Availability Statement: The data presented in this study are available on request from the corresponding author. The data are not publicly available due to privacy issues.

Acknowledgments: Karol M. Golasiński acknowledges the support of the Japan Society for the Promotion of Science (JSPS) Postdoctoral Fellowship (ID No. P20812). This research was funded in part by the National Science Centre, Poland through the Grant 2023/48/C/ST8/00038. The authors would like to express their gratitude to Leszek Urbański from IPPT PAN for conducting tensile tests.

Conflicts of Interest: The authors declare no conflicts of interest. The funders had no role in the design of the study; in the collection, analyses, or interpretation of data; in the writing of the manuscript; or in the decision to publish the results.

References

1. Kim, H.Y.; Satoru, H.; Kim, J.I.; Hosoda, H.; Miyazaki, S. Mechanical properties and shape memory behavior of Ti-Nb alloys, *Mater. Trans.* **2004**, 452443e2448. https://doi.org/10.2320/matertrans.45.2443.
2. Kim, H.Y.; Ikehara, Y.; Kim, J.I.; Hosoda, H.; Miyazaki, S. Martensitic transformation, shape memory effect and superelasticity of Ti–Nb binary alloys, *Acta Mater.* **2006**, 54 2419 – 2429. https://doi.org/10.1016/j.actamat.2006.01.019.
3. Tahara, M.; Kim, H.Y.; Inamura, T.; Hosoda, H.; Miyazaki, S. Role of interstitial atoms in the microstructure and non-linear elastic deformation behavior of Ti–Nb alloy, *J. Alloys Compd.* **2013**, 577, S404 – S407, https://doi.org/10.1016/j.jallcom.2011.12.113.
4. Tahara, M.; Kim, H.Y.; Hosoda, H.; Miyazaki, S. Shape memory effect and cyclic deformation behavior of Ti–Nb–N alloys, *Funct. Mater. Lett.* **2009**, 2, 79 – 82, https://doi.org/10.1142/S1793604709000600.
5. Miyazaki, S. My Experience with Ti–Ni-Based and Ti-Based Shape Memory Alloys. *Shap. Mem. Superelasticity.* **2017**, 3, 279 – 314. https://doi.org/10.1007/s40830-017-0122-3.
6. Golasiński, K.; Maj, M.; Tasaki, W.; Pieczyska, E.A.; Kim, H.Y. Full-Field Deformation Study of Ti–25Nb, Ti–25Nb–0.3O and Ti–25Nb–0.7O Shape Memory Alloys During Tension Using Digital Image Correlation, *Metall. Mater. Trans. A.* **2024**, 55, 2509 – 2518. https://doi.org/10.1007/s11661-024-07414-8.
7. Nowak, M.; Maj, M. Determination of coupled mechanical and thermal fields using 2D digital image correlation and infrared thermography: Numerical procedures and results, *Archiv. Civ. Mech. Eng.* **2018**, 18, 630 – 644, https://doi.org/10.1016/j.acme.2017.10.005.
8. Golasiński, K.M.; Pieczyska, E.A.; Staszczak, M.; Maj, M.; Furuta, T.; Kuramoto, S. Infrared thermography applied for experimental investigation of thermomechanical couplings in Gum Metal, *Quant. InfraRed Thermogr. J.* **2017**, 14, 226 – 233, https://doi.org/10.1080/17686733.2017.1284295.
9. Golasiński, K.M.; Maj, M.; Urbański, L.; Staszczak, M.; Gradys, A.; Pieczyska, E.A. Experimental study of thermomechanical behaviour of Gum Metal during cyclic tensile loadings: the quantitative contribution of IRT and DIC, *Quant. InfraRed Thermogr. J.* **2023**, 21, 259 – 276. https://doi.org/10.1080/17686733.2023.2205762.
10. Tobe, H; Kim, H.Y.; Inamura, T; Hosoda, H; Miyazaki, S. Origin of {332} twinning in metastable β-Ti alloys, *Acta Mater.* **2014**, 64, 345 – 355. https://doi.org/10.1016/j.actamat.2013.10.048.